

Design procedure for prestressed concrete beams

Piero Colajanni^a, Antonino Recupero^b and Nino Spinella^{*}

*Dipartimento di Ingegneria Civile, Informatica, Edile, Ambientale e Matematica Applicata,
Università di Messina, Messina, Italy*

(Received November 14, 2012, Revised September 3, 2013, Accepted September 16, 2013)

Abstract. The theoretical basis and the main results of a design procedure, which attempts to provide the optimal layout of ordinary reinforcement in prestressed concrete beams, subjected to bending moment and shear force are presented. The difficulties encountered in simulating the actual behaviour of prestressed concrete beam in presence of coupled forces bending moment - shear force are discussed; particular emphasis is put on plastic models and stress fields approaches. A unified model for reinforced and prestressed concrete beams under axial force - bending moment - shear force interaction is provided. This analytical model is validated against both experimental results collected in literature and nonlinear numerical analyses. Finally, for illustrating the applicability of the proposed procedure, an example of design for a full-scale prestressed concrete beam is shown.

Keywords: shear, flexure, prestressed concrete, design, plasticity

1. Introduction

In the last forty years, theoretical and experimental investigations have clarified the most important aspects of shear failure in Reinforced Concrete (RC) element (Nielsen, 1984; Vecchio and Collins, 1986, Collins *et al.* 1996; Russo and Puleri 1997, Russo *et al.* 2004, Russo *et al.* 2005) and many models to predict the shear and flexural capacity of Prestressed Concrete (PC) beams are available in literature (Au *et al.* 2009, Ahn *et al.* 2010, Au *et al.* 2011, Gocic and Sadovic 2012). However, little consensus as developed among researchers as to which is the most accurate and suited for use in design. Moreover, historically, the many of codes propose two different models, for RC structures on one side and for PC elements from the other (ACI Committee 318, 1983, Eurocode 2 2002).

The procedure to design RC elements subjected to shear (V) and bending moment (M) reflects the classical truss model approach. The idea to use truss models of following the flow of stresses goes back to Ritter (1989). Based on careful observations of structure behaviour as well as a systematic understanding of basic principles of structural mechanics, Mörsch (1908) has greatly advanced this concept and introduced the classical 45° truss model, whose simplicity and clearness

^{*}Corresponding author, Ph.D., E-mail: nino.spinella@unime.it

^aAssociate Professor, e-mail: pcolajanni@unime.it

^bAssistant Professor, e-mail: antonino.recupero@unime.it

are striking even today.

The application of the theory of plasticity to structural concrete beams and walls started in the late 1950s. Basic work, in this field, was mainly carried out by two groups of researchers around Thürlimann (1983) and Nielsen (1984). Their contribution tries to provide an overview on limit analysis methods for structural concrete beams subjected to shear and bending moment and to give a structure at the considerable provisions of Eurocode (2002).

Though sophisticated Non-Linear Finite Element Analysis (NLFEA) can be nowadays performed using accurate models (Vecchio and Collins 1986, Bertagnoli *et al.* 2011), simplified mechanical models are still definitely needed, at the aim to speed up the design and the analysis.

In the case of RC elements, by using the truss models and the stress field theory, a model to evaluate the shear strength in presence of axial force has been proposed and discussed by several authors, referring to rectangular cross sections (Fanti and Mancini, 1995), to T or I-shaped cross sections (Recupero *et al.* 2003), and to circular cross sections (Rossi and Recupero 2013). This model was also generalized in presence of Fibres Reinforced Concrete (FRC) (Colajanni *et al.* 2008a, Spinella *et al.* 2010, Colajanni *et al.* 2012, Cucchiara *et al.* 2012, Spinella 2013, Foster *et al.* 2013).

An analytical model for evaluation of the N-M-V interaction domain of RC and PC elements by means of a unified simplified approach was proposed in (Recupero *et al.* 2005). It has been derived as the generalization of the series of previously mentioned models based on the stress-fields approach.

This simplified approach assumes compressive stress field in the concrete, and equivalent uniformly distributed tensile stresses, corresponding to the action of the stirrups. In this model the inclination angle θ of the compressive stresses may be different from 45° degrees; as a matter of fact it varies as the shear force increases after yielding of web reinforcements.

Since any analysis exploiting the potential of the proposed approach has not yet been developed, in this paper a study concerning the optimization of steel reinforcement layouts of PC elements is carried out, and a procedure for choosing the layouts is proposed.

To illustrate the applicability of the proposed procedure, a design example of a bridge PC beam is shown. Finally, the beam, designed by this procedure, is virtually loaded up to failure by a nonlinear FEM code VecTor (Wong and Vecchio 2002), a well known and reliable code based on the Modified Compression Field Theory (MCFT) (Vecchio and Collins 1986). Preliminarily, the effectiveness of both the design model and the FEM code will be proved against results of experimental tests collected in literature.

2. Review of the analytical model

The sectional analytical model described in detail in (Recupero *et al.* 2005) is herein used to provide the shear-flexure strength of PC beams. It allows to take into account the simultaneous presence of bending moment and shear force on the beam including the effect of prestressed tendons.

The load-carrying capacity of a beam is evaluated by using a simplified layered model, in which the tensile contribution of concrete is neglected, flanges and the part of the web are assumed to resist to normal stress only, while the remaining central part of web is able to resist both to normal stress and shear stress also (Fig. 1a). The flanges and the portion of the web at the top and the bottom of the cross-section, having depth (z_1) and (z_2) respectively are subjected to uniform

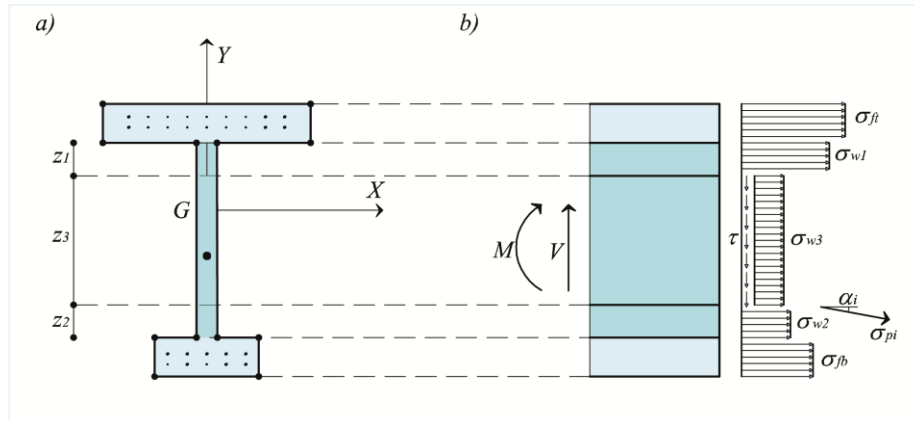


Fig. 1 a) Geometrical model of the beam; b) internal and external forces scheme assumed

stress fields in the longitudinal direction. The remaining part of the web, having a depth equal to z_3 , is also subjected to a uniform stress field inclined to the longitudinal direction of the beam by a variable θ angle, due to the shear stresses along cracks. Longitudinal reinforcements of the beam can be distributed along the entire depth of cross-section (flanges and web), while the transversal reinforcements is considered only on the web. Both reinforcements give uniform stress fields (Fig. 1b).

Summarizing, normal stresses in concrete and steel rebars in top and bottom flange σ_{tff} , σ_{tbf} and in ending portions of web σ_{w1} , and σ_{w2} , contribute to the axial compression, while the normal and shear stresses σ_{w3} and τ along the inner part of web represent actions in the inclined concrete strut and the stress fields due to transversal and skin reinforcements.

The analytical model allows in predicting the beam failure, which can occur either by concrete crushing or by reinforcement yielding. The ultimate strength and mode of collapse are obtained considering a linear domain defined by different limit conditions on the axial and shear stresses in the flanges and outermost web layers, and in the central web layer, which also take into account the geometrical percentage of reinforcement (ρ_{tf} , ρ_{bf} , ρ_w , ρ_{tw}), and the design value of steel yielding and compression strength (f_{yd} , f_{cd1} , f_{cd2}) (Eurocode 2002). The axial forces due to prestressing tendons (σ_{pi}), acting along a direction inclined by an angle to the longitudinal axis of the beam, are also limited to the design value (f_{pd}).

Furthermore, some geometrical conditions have to be satisfied. They concern the positive value of web portion depth (z_1 , z_2 , z_3) and their minimum values. In particular, the central web layer depth (z_3) must be large enough to carry on shear stresses. A numerical integration procedure along all layers (Recupero *et al.*, 2005) allows calculation of the resultants of the axial and shear stresses, including the forces acting on the prestressing tendons, thus their sum provide the internal resisting force of the cross-section in terms of design resistant bending moment (M_{Rd}) and design resistant shear force (V_{Rd}). A resume of equations involved is reported in Appendix A.

The best outcome of the mathematical model is given by a linear programming method that allows one to evaluate both the depth of the web layers and all stresses by maximizing the element resisting action in the respect of the plastic admissible conditions on material strengths and geometrical restrains on the layer sizes.

3. Finite element model

To validate the efficiency of the analytical model and the proposed design procedure, the responses of the specimens that will be designed in this research work will be evaluated by sophisticated nonlinear tools. The NLFEA will be also validated by reproducing the response of some experimental tests collected in literature.

The NLFEA allows one to obtain information about the behaviour of structural member considered. They concern stress and strain conditions at different load stages, providing a wide and accurate analytical reproduction of tests.

To reproduce the response of RC elements subject to different load conditions, several analytical formulations have been proposed in literature, which adopt theoretical models based on several constitutive laws and mechanical theories. The theoretical models taken into account in the NLFEA utilized herein are the MCFT and the Disturbed Stress Field Model (DSFM), which represent general models for the load-deformation behaviour of two-dimensional cracked RC subjected to shear and flexure (Vecchio and Collins 1986). The concrete stresses in the principal directions are summed with rebar stresses which are assumed to act along rebar longitudinal axis only. The concrete constitutive behaviour both in compression and tension has been originally derived from wide experimental survey performed by Vecchio and Collins (1982).

The basic assumption of the MCFT is that the principal strain directions coincide with the principal stress directions. This assumption has recently been removed by Vecchio (2000) which has introduced the DSFM. The DSFM explicitly incorporates rigid slipping along crack surfaces into the compatibility relations for the element, allowing for a divergence between inclination angles of average principal stress and apparent average principal strain in the concrete. In addition, MCFT and DSFM have been recently extended to the case of fibrous concrete elements (Colajanni *et al.* 2008b, Spinella *et al.* 2012), proving the ability to reproduce the response of structural members with different mechanical and load conditions.

In the MCFT the compatibility conditions linking the strains in the cracked concrete with the strains in the rebars are expressed in terms of average strains, where the strains are measured over base lengths that are greater than the crack spacing. The equilibrium conditions, which link the concrete stresses and the rebars stresses to the applied loads, are also expressed in terms of average stresses.

In the same way, the strains used for the stress-strain relationships are average strains, thus they consider together the combined effects of local strains at cracks, strains between cracks, bond-slip, and crack slip. The calculated stresses are also average stresses in that they implicitly encompass the stresses between cracks, stresses at cracks, interface shear on cracks and dowel action. In this model, the cracked concrete in RC is treated as a different material with empirically defined constitutive law. This constitutive behaviour can differ from the traditional stress-strain curve of a standard cylinder, for example.

The equilibrium equations, the compatibility relationships, the rebars stress-strain relationships, and the stress-strain relationships for the cracked concrete in compression and tension enable the average stresses, the average strains, and the angle to be determined for each load level up to failure.

As can be deduced from the above, the MCFT and DSFM are powerful and general tools for the NLFEA of RC elements, and for these reasons it has been chosen to perform several numerical analyses.

4. Experimental validation of analytical and fem models

4.1 Experimental tests by literature

The analytical model was validated against several experimental data collected from the literature. Herein, tests on PC beams performed by Tan and Ng (1998) are taken into account. As shown in Fig. 2, the specimens have a length between 1200 and 3000 mm, the T-shaped cross section is 300 mm in depth, and they are externally prestressed with straight tendons. The beams were identified by the codes ST-1, ST-2, ST-2C, ST-2C+, ST-2S, ST-2P, and ST-3. They were designed with different concrete strengths, internal reinforcement, and span as test parameters. Beam ST-2 served as a reference beam. Beam ST-2C and ST-2C+ were similar to ST-2 except for the concrete strength. Beam ST-2S had lesser shear reinforcement in the form of vertical stirrups while beam ST-2P was subjected to a midspan load; otherwise they were the same as beam ST-2. Beams ST-1 and ST-3 differed from beam ST-2 only in shear span, which was one-third of the effective span in each beam. Each beam was provided with a 100 mm wide deviator at midspan. Except for beam ST-2C+, the internal longitudinal steel reinforcement consisted of two high-yield deformed steel bars, 16 mm in nominal diameter (designated as T16 bars), at the bottom and four mild steel bars, 8 mm in diameter, at the top, with average yield strength of 530 MPa and 338 MPa respectively. In beam ST-2C+, two high-yield deformed steel bars with a diameter of 20 mm and an average yield strength of 460 MPa were used as the bottom longitudinal reinforcement instead.

Transverse reinforcement consisting of R8 mild steel stirrups was provided throughout the length of all beams except ST-3 where mild steel stirrups with a diameter of 6 mm and average

Table 1 Dimensions and reinforcement details of beams tested by Tan and Ng (1998)

Specimen	B1	B2
ST-1	0.852	0.883
ST-2	0.898	0.929
ST-2C	0.961	0.994
ST-2C+	0.935	1.005
ST-2S	0.734	0.755
ST-2P	0.878	0.909
ST-3	0.957	0.986
Mean	0.888	0.923
Standard deviation	0.079	0.087

Table 2 Numerical versus experimental ratios for beams tested by Tan and Ng (1998)

Specimen	B1	B2
ST-1	0.852	0.883
ST-2	0.898	0.929
ST-2C	0.961	0.994
ST-2C+	0.935	1.005
ST-2S	0.734	0.755
ST-2P	0.878	0.909
ST-3	0.957	0.986
Mean	0.888	0.923
Standard deviation	0.079	0.087

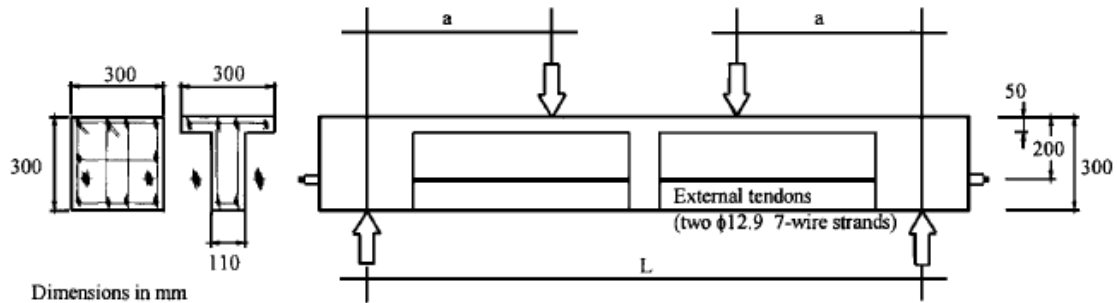


Fig. 2 Geometrical setup of specimens tested by Tan and Ng (1998)

yield strength of 300 MPa were used. The spacing of the stirrups was 200 mm within the constant moment region. Within the shear spans, the spacing was 50 mm for beam ST-3, 200 mm for beam ST-2S and 75 mm for other beams (Tab. 1).

The comparison of the model prediction against test results is carried out neglecting the safety coefficient proposed by Eurocode (2002) for uniaxial concrete strength f_{cd1} and for stresses in presence of shear f_{cd2} . For the latter the effectiveness shear factor is assumed equal to 0.70 and the partial safety factor for concrete is set equal to 1 [i.e. $f_{cd1} = (1 - f_{ck}/250)f_{ck}$; $f_{cd2} = 0.7(1 - f_{ck}/250)f_{ck}$].

With the aim to compare the performances achieved by the analytical model with different assumptions, two different web depths are considered: in the first case it is equal to net web depth (B1); in the second one it is extended to the position of the bottom reinforcement in the flange (B2). These choices reflect the fact that the shear resisting portion of web is not rigorously defined. In Table 2, the ratios between analytical and experimental results are reported. They show that the analytical model provides conservative prediction of the load-carrying capacity of specimens, with the best performance achieved adopting the depth web extended up to the bottom longitudinal reinforcement (B2). Thus, it confirms that the physical procedure is adequate to reproduce the experimental results.

4.2 Fe modeling of specimens and load conditions

The specimens of survey tests carried out by Tan and Ng (1998), as described in the previous section, are modelled developing a two-dimensional plane stress model, suitably restrained to the symmetrical axis (Fig. 3). The mesh is composed of four-node rectangular elements 50×25 , 50×35 , and 50×50 mm in size with uniform thickness to represent the concrete (each region of the beam is identified by a different colour), and two-nodes truss bars with uniform cross-sectional area for longitudinal reinforcement. To take into account the action of prestressing cable, an equivalent nodal force is evaluated by simple geometric considerations and applied at the beam (Fig. 3). The finite element size is chosen adopting the cover as vertical size and a ratio between sides of rectangular element close to one. Sliding between rebar and concrete is neglected, and then perfect steel-to-concrete bond is therefore assumed (Spinella *et al.* 2012).

According to experimental procedure followed by Tan and Ng (1998), support and point loads were modelled as concentrate nodal actions on steel plates with a thickness of 25 mm, fully connected to concrete.

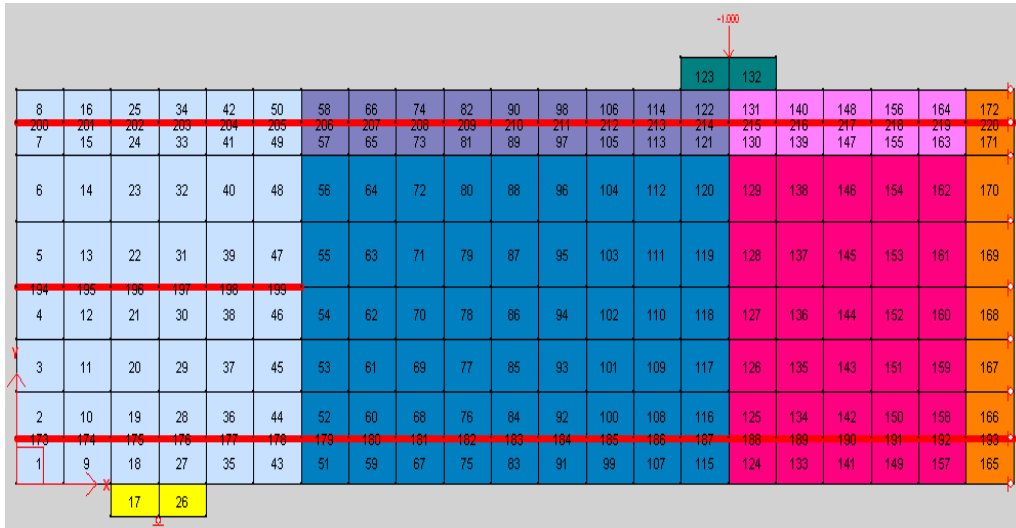


Fig. 3 Two-dimensional mesh model for specimen ST-2

Numerical analyses are performed assigning three different load patterns acting respectively, in sequence: a static self weight on all concrete elements; a static nodal force equivalent to the effect of prestressing cable, applied to the free side of the beam; and a monotonically increasing displacement, co-axial to the effective transversal load, on the node located in the middle of the steel transfer load plate. The total load is computed as twice the reaction force at the support. Thus, the displacement controlled procedure is able to reproduce the post-peak branch of the load-displacement curve.

The software that implements the MCFT allows managing many parameters concerning mechanical characteristics of materials and their constitutive laws. The numerical analyses are carried out assuming the default values for each parameter, and specifically taking the Hognestad parabola for concrete, and the elastic-plastic law for steel rebars.

4.3 Comparison of results by fem analysis

Figs. 4-6 illustrate the load-displacement numerical curves for the considered beams. The experimental curves are represented by smooth solid lines, while in each curve provided by the NLFEA, a different symbol is added. Furthermore, in the same graph, the load capacity (P_{ani}) for each specimens obtained by analytical model is plotted by a straight dashed line and reported in a small table also.

The numerical curves show the ability of MCFT to capture the stiffness of those specimens and to estimate load capacity and ultimate deflection (Tab. 3). Moreover, the slope of some numerical curves is slightly more inclined than the slope of experimental curves, mainly at the beginning of the non-linear branch, probably due to the effect of tension stiffening modelling, which plays an important role at the onset of cracking.

Finally, it can be underlined as the estimate of ultimate capacity, formulated by analytical model as based on plastic approach, is always on the safety side.

Table 3 FEM and experimental results for beams tested by Tan and Ng (1998)

Specimen	P_{FEM}	P_{exp}	P_{FEM}/P_{exp}
ST-1	373.6	385.0	0.97
ST-2	307.2	310.2	0.99
ST-2C	301.8	299.6	1.01
ST-2C+	303.0	270.5	1.12
ST-2S	309.8	300.0	1.03
ST-2P	356.4	331.1	1.08
ST-3	186.8	186.8	1.00
Mean	/	/	1.03
Standard deviation	/	/	0.05

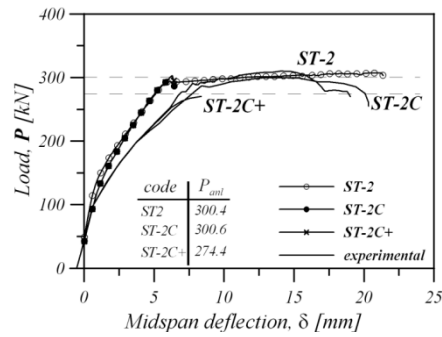


Fig. 4 Analytical versus experimental load-displacement curves for ST-2, ST-2C, and ST-2C+ beams

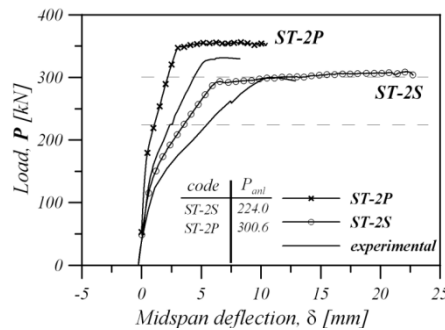


Fig. 5 Analytical versus experimental load-displacement curves for ST-2P and ST-2S beams

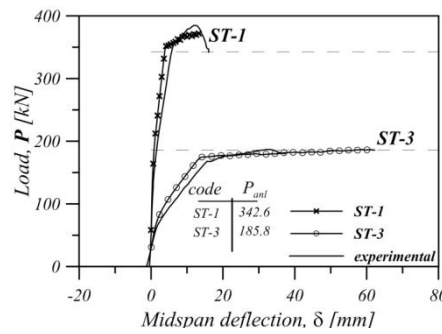


Fig. 6 Analytical versus experimental load-displacement curves for ST-1 and ST-3 beams

5. Proposed design procedure

The proposed procedure to design PC structural elements is powerful and flexible. It allows one to evaluate the interaction between the principal parameters that govern the physical phenomena. In fact, after defined the prestressing reinforcement ratio and the longitudinal and transversal web reinforcement on the basis of the criteria that will be explained afterwards, the interaction between bending moment, flange reinforcement and shear can be completely evaluated.

In Fig. 7, a design chart for the design of total longitudinal flange reinforcement mechanical ratio ω_{fl} , derived from the normalized interaction domain for the beam ST1 is plotted. It shows the curves of the longitudinal flange reinforcement mechanical ratio ω_{fl} needed to obtain a given value of the normalized design bending moment m_{sd} ; the curves prove that that flange reinforcement does not contribute to the strength of beam for normalized bending moment close to 1/10. By varying the bending moment, the shear strength increases with the increase of the flange reinforcement. Thus, this design chart is a strong and useful tool both in the preliminary design, to understand the magnitudes of force involved, and in the final check, to optimize the longitudinal reinforcement ratio of the structural element in order to contribute to the shear strength also.

In first step, the cross-section shape, dimensions and the layout of the prestressing reinforcements should be designed by governing or limiting deflection, cracking and compression stresses for service limit state (SLS) stages, as appropriate, in accordance with the code requirements. The cracking of a beam under service conditions should be controlled, with limits on crack width being selected to ensure acceptable appearance and durability.

In second step, once the size of the prestressing reinforcement ratio has been settled, the design of ordinary additional reinforcement, in longitudinal and transversal direction are performed by control of ultimate limit states (ULS). The longitudinal reinforcement can be placed both in the flanges and in the web (as skin reinforcement), the transversal reinforcement in form of stirrups is placed in the web. Generally, several configurations of longitudinal (ω_l) and transversal (ω_w) reinforcements are admissible in the web. In fact, when longitudinal web reinforcement (ω_w) increases the transversal reinforcement decreases (ω_w) and *vice versa*. Therefore, the designer can choose, among the different configurations that are allowable, the more convenient for practical and economical requirements. These concepts are graphically explained in the design charts depicted in Figs. 8-9. They are useful tools that allows the selection of more proper configuration, among the different ones, by providing the optimal reinforcement web layout for several values of total longitudinal flange reinforcement (ω_{fl}).

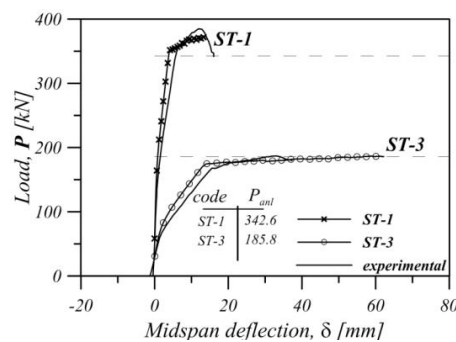
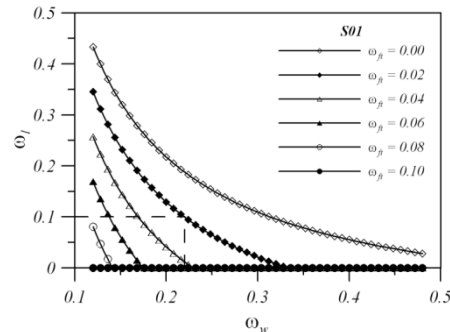
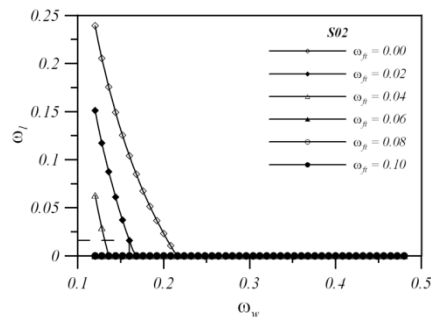


Fig. 7 Design chart ($m_{sd}-\omega_{fl}$) for the ST-1 beam

Fig. 8 Interaction domain (ω_l - ω_w) for section S01 of full-scale bridge beamFig. 9 Interaction domain (ω_l - ω_w) for section S02 of full-scale bridge beam

5.1 Example: design of a full scale bridge beam

The design procedure described in the previous sections is herein used to perform the design of a full scale bridge beam, showing the ability of proposed procedure to optimize the amount of skin reinforcement and stirrups along the web to resist at shear and bending moment. As better described forward, a new value of mechanical percentage of stirrups has been assumed for each regions of PC beam, then a value of mechanical percentage of skin reinforcement has evaluated for a given value of mechanical percentage of flanges reinforcement.

Fig. 10 shows the actual views of bridge taken into account. It consists of seven double “T” PC beam with single span $L = 34.60$ m and a RC deck with thick of 200 m. The final load was estimated considering the following design values: deck weight (93 kN/m); PC beams weight (139.5 kN/m); transversal RC diaphragms weight (10.5 kN/m); guard rails (6 kN/m); handrails (2.25 kN/m); and flooring (40.5 kN/m). The sum of static loads was divided for the number of PC beams to obtain $q_s = 291.8/7 = 41.7$ kN/m. The traffic loads provide a design dynamic equivalent load (q_d) on the lateral PC beam equal to 22.9 kN/m. Finally, the total design load on a single PC beam is $q_{tot} = q_s + q_d = 40.5 + 22.9 = 64.6$ kN/m. In Fig. 11, the transversal section of bridge is represented, and in Fig. 12 the prestressing reinforcement setup of PC beam is plotted.

The PC beam was previously designed following two phases: firstly, calculating the prestressing force of cables needed to avoid cracks at the SLS; then, estimating the longitudinal reinforcement amount of flanges and the transversal reinforcement amount to resist at the shear force and the bending moment at the ULS. Finally, the minimum skin reinforcement gave by the

code was spread along the web of the beam.

The schematic layout of PC beam and prestressing reinforcement forces of half beam is shown in Fig. 13 (considering the symmetry of the structure) where the prestressing normal force (in kN) due to strands is represented by arrows in correspondence of the cross-section where it is completely developed. The geometrical percentage reinforcement is summarized in Table 4, where ρ_{sx} and ρ_{sy} are the geometric percentage of reinforcement, in x (longitudinal) and in y direction (transversal), for original (a) and optimized (b) beam setup, respectively; z and t are the depth and the thickness in mm of the cross-section along the longitudinal axis of the beam, respectively; finally, R_i ($i = 1, 2, 3, 4$) is the generic region of length l (mm) in which the PC beam is ideally sliced.

At the aim to optimize the reinforcement of PC beam, the design procedure described in the previous sections is used considering some cross-sections along the longitudinal axis of the PC beam and the related mechanical and geometrical characteristics, as well as the different stress states. The control cross-sections of beam are chosen with narrow pitch in the vicinity of the support, where the shear force is relevant, and with wider pitch in the central part of the beam.

The beam is pinned at the support, the total distributed load ($q_{tot} = 64.6 \text{ kN/m}$) is smeared along the deck as an equivalent volume weight; finally, an external vertical displacement applied at one quarter of the span length (Kani 1967) will be monotonically incremented until the PC beam crisis. This load scheme allows to simply calculating all forces in each cross-sections of the beam; thus the sectional method can be used to evaluate the design amounts of stirrups and longitudinal web reinforcement assuming a constant amount of longitudinal reinforcement in the flanges.

The Figs. 8 and 9 show the design charts relating the mechanical percentage of longitudinal web reinforcement (ω_l) and the mechanical percentage of transversal reinforcement (ω_w), for several values of mechanical percentage of flanges reinforcement (ω_f), evaluated in correspondence of section S01 (close to the support) and S02 (two meters far from the support), respectively (Fig. 13). The curves show the interaction between longitudinal web reinforcement and stirrups, which tends to flatten out with the increase of ω_f and the shift of the cross-section far from the support. The former is due to the rule of longitudinal flange reinforcement to resist at normal stress (normal force and bending moment); the latter is due to the action of cables which provides an internal bending moment that tends to balance the external bending moment.



(a)



(b)

Fig. 10 (a) Longitudinal and (b) transversal view of bridge

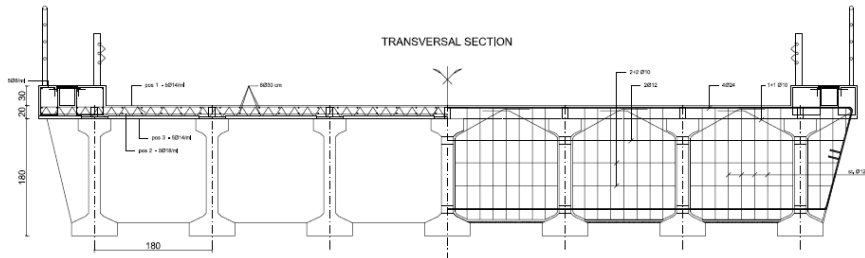


Fig. 11 Transversal section scheme of bridge (dimensions in cm)

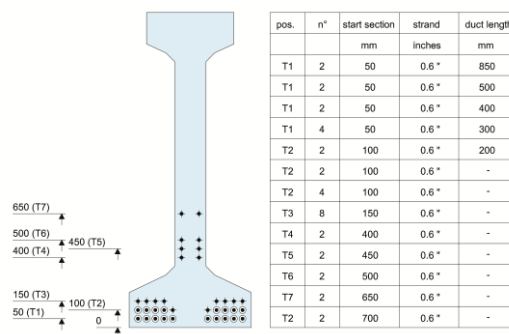


Fig. 12 Prestressing reinforcement setup of PC beam

Table 4 a) Original; and b) optimized geometrical reinforcement of full-scale bridge beam

	R1		R2		R3		R4	
	l = 3000 mm		l = 5000 mm		l = 3500 mm		l = 5800 mm	
	ρ_{sx} (%)	ρ_{sy} (%)						
S								
$z = 200$ mm	0.096	0.040	0.096	0.040	0.096	0.040	0.096	0.040
$t = 1800$ mm								
Top								
$z = 200$ mm	0.905	0.113	0.905	0.113	0.101	0.057	0.101	0.057
$t = 500$ mm								
Web								
$z = 1300$ mm	a) 0.172	a) 1.257	a) 0.172	a) 0.873	a) 0.172	a) 0.436	a) 0.172	a) 0.279
$t = 180$ mm	b) 0.395	b) 0.873	b) 0.079	b) 0.873	b) 0.079	b) 0.873	b) 0.079	b) 0.436
Bottom								
$z = 300$ mm	0.096	0.081	0.096	0.081	0.096	0.040	0.096	0.040
$t = 700$ mm								

Assuming a value of mechanical percentage of stirrups, the correspondent value of mechanical percentage of skin reinforcement is easily evaluated for a given value of mechanical percentage of flanges reinforcement (ω_f). In the case taken into account, at $\omega_w = 0.22$ and for $\omega_f = 0.02$, the minimum value of $\omega_l = 0.10$ is obtained for the cross-section close to the support. This minimum value of mechanical percentage skin reinforcement corresponds at ten longitudinal rebars in 12 mm of diameter along the two sides of the web, and considering the mechanical properties of concrete ($f_{cd2} = 14.8$ MPa) and steel ($f_{yd} = 373.9$ MPa) the geometrical percentage of skin

reinforcement is $\rho_{sx} = 0.395\%$, while for transversal reinforcement two stirrups with two legs in 10 mm of diameter is used. In the same way it can proceed to the design of other cross-sections can be performed, obtaining the optimized setup scheme of web reinforcement (b) summarized in Table 4. The optimized scheme shows as the reinforcement is homogeneous along the entire web and in both the orthogonal directions.

As for the specimens of Tan and Ng (1998), the considered full scale bridge beam is now analyzed by the NLFEA. The modelling technique used is the same described in the previous sections, and in Fig. 14a the adopted mesh is shown and indicating with a different colour each region of the beam. The two-dimensional plane stress model is suitably restrained to the symmetrical axis and the mesh is composed of four-node rectangular elements 200×260 mm in size with uniform thickness to represent the concrete, and two-nodes truss bars with uniform cross-sectional area for longitudinal reinforcement. Also in this case, the numerical analyses are performed assigning three different load cases acting in succession. Several static nodal loads equivalent to the action of prestressing cable are applied to the free side of the beam representing the normal force due to the cables. The Fig. 15 shows the $P-\delta$ curves evaluated by the NLFEA of the beam as originally designed and as herein optimized in the web reinforcement, respectively. The target load on half beam is $P = q_{tot} L/2 = 1124.5$ kN. The curve that represents the numerical analysis of the original scheme beam provides a load capacity of 1267.1 kN that is 13% greater than target value. The numerical analysis of the optimized scheme beam provides a load capacity of 1147.8 kN that is 2% larger than target, thus, a value closer to the target is obtained. This layout is more advantageous and cheaper than the original one, without any degradation of performance, as showed by the crack pattern obtained by FEM analysis (Fig. 14b).

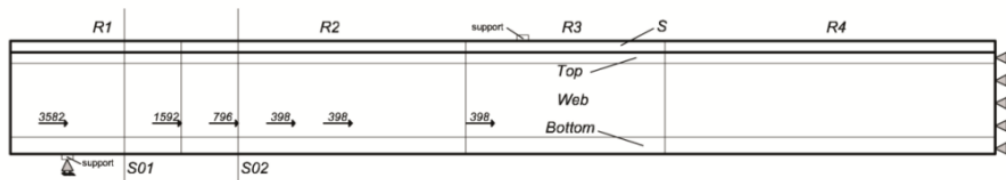


Fig. 13 Schematic layout of PC beam and prestressing reinforcement forces

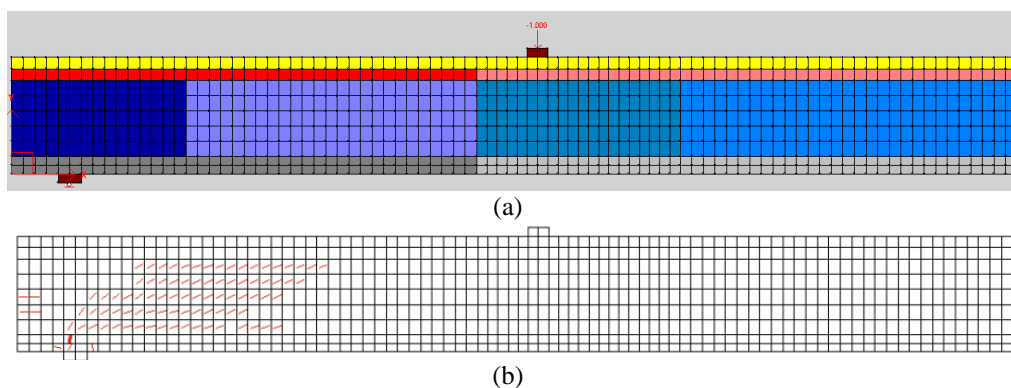


Fig. 14 (a) Two-dimensional mesh model and (b) crack pattern for full-scale bridge beam

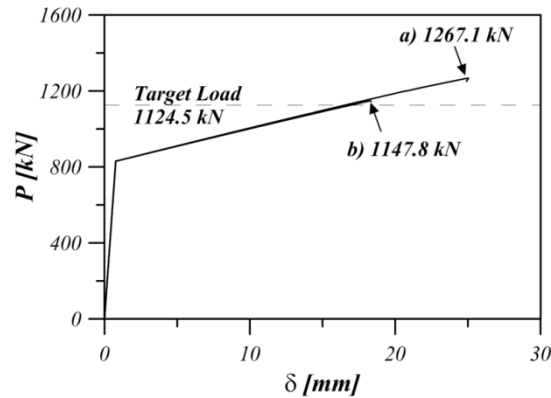


Fig. 15 Analytical load-displacement curve for (a) original and (b) optimized full-scale bridge beam

6. Conclusions

Many models are available in predicting the shear strength of PC beams in literature, and historically, the large majority of technical papers and codes propose two different models for reinforced concrete structures on one side and for prestressed elements from the other.

In this paper a unified model, already proposed by the same authors, was scrutinized and discussed. The model is effective both for RC and for PC elements and, differently from those existing in literature, is able of taking in account the effects of axial force, bending moment, and shear force interaction.

In this work, the characteristics of the model were analyzed and its effectiveness is proved by favourable comparison against the results of experimental tests collected in literature. The results showed that the proposed model provide a straightforward safe assessment of the ultimate load with and is a handy tools for design and verification of element strength.

Finally, a procedure for reinforcement design optimization of PC beam was proposed and applied to a case of study. A full-scale PC beam of an existing bridge was redesigned, obtaining a more advantageous and cheaper configuration than original one. The two specimens are virtually conducted up to collapse by a NLFEA. showing the effectiveness of the proposed procedure.

Additional efforts are needed in order to analyze beams with different cross-section shapes and reinforcement setup to confirm the generality of the proposed model.

References

- ACI Committee 318 – (1983), “Building code requirements for reinforced concrete (ACI 318-95) and commentary ACI 318 R-95” - *American Concrete Institute*, Detroit.
- Ahn, J.H., Jung, C.Y. and Kim, S.H. (2010), “Evaluation on structural behaviors of prestressed composite beams using external prestressing member”, *Struct. Eng. Mech.*, **34**(2), 247-275.
- Au, F.T.K., Leung, C.C.Y., Kwan, A.K.H. and Du, J.S. (2009), “Flexural ductility of prestressed concrete beams with unbonded tendons”, *Comput. Concr.*, **6**(6),451-472.
- Au, F.T.K., Leung, C.C.Y. and Kwan, A.K.H. (2011), “Flexural ductility and deformability of reinforced and prestressed concrete sections”, *Comput. Concr.*, **8**(4),473-489.
- Bertagnoli, G., Mancini, G., Recupero, A. and Spinella, N. (2011), “Rotating compression field model for

- reinforced concrete beams under prevalent shear actions”, *Struct. Concrete*, **12**(3), 178-186
- Colajanni, P., Recupero, A. and Spinella, N. (2008a), “Shear strength prediction by modified plasticity theory for SFRC beams”, *2008 Seismic Engineering International Conference Commemorating the 1908 Messina and Reggio Calabria Earthquake, MERCEA 2008*; Reggio Calabria, Italy; 8-11 July 2008, **1020**(1), 888-895.
- Colajanni P., La Mendola L., Priolo S. and Spinella N. (2008b), “Experimental tests and FEM model for SFRC beams under flexural and shear loads”, *2008 Seismic Engineering International Conference Commemorating the 1908 Messina and Reggio Calabria Earthquake, MERCEA 2008*; Reggio Calabria, Italy; 8-11 July 2008, **1020**(1), 872-879.
- Colajanni P., Recupero A. and Spinella N. (2012), “Generalization of shear truss model to the case of SFRC beams with stirrups”, *Comput. Concr.*, **9**(3), 227-244.
- Collins M.P., Mitchell D., Adebar P.E. and Vecchio F.J. (1996), “A general shear design method”, *ACI Struct. J.*, **93**(1), 36-45.
- Cucchiara C., Fossetti M. and Papia M. (2012), “Steel fibre and transverse reinforcement effects on the behaviour of high strength concrete beams”, *Struct. Eng. Mech.*, **42**(4), 551-570.
- “Design of Concrete Structures – Part.1 : General Rules and Rules for Buildings – prEN 1992-1-1 (Revised final draft)” April 2002.
- Fanti G. and Mancini G. (1995), “Shear, normal force, bending moment interaction in bridge piers”, *Proceedings of the First Japan -Italy Workshop on Seismic Design and Retrofit of Bridges*, March 13-14, 1995 Tsukuba, Japan.
- Foster S.J., Htut T. and Ng T.S. (2013), “High performance fibre reinforced concrete: Fundamental behaviour and modelling”, *8th International Conference on Fracture Mechanics of Concrete and Concrete Structures, FraMCoS 2013*; Toledo; Spain; 11-14 March 2013, pages 69-78
- Gocic, M. and Sadovic, E. (2012), “Software for application of newton-raphson method in estimation of strains in prestressed concrete girders”, *Comput. Concr.*, **10**(2), 121-133.
- Kani, G.N.J. (1967), “How safe are our large reinforced concrete beams?”, *ACI Struct. J.*, **64**(4), 128-141.
- Mörsch, E. (1908), “Der Eisenbetonbau. Seine Theorie und Anwendung”, 3rd, rev. ed., Stuttgart: Wittwer.
- Nielsen, M.P. (1984), “Limit analysis and concrete plasticity”, Prentice-Hall, Englewood Cliffs, NJ.
- Recupero A., D’Aveni A. and Ghersi A. (2003), “N-M-V Interaction domains for box and I-shaped reinforced concrete members”, *ACI Struct. J.*, **100**(1), 113-119.
- Recupero, A., D’Aveni, A. and Ghersi A. (2005), “Bending Moment - Shear Force Interaction Domains for Prestressed Concrete Beams”, *ASCE J. Struct. Eng.*, **131**(9), 1413-1421.
- Ritter W. (1989), “Die bauweise hennebique (Construction Techniques of Hennebique),” *Schweizerische Bauzeitung, Zürich*, **33**(7), 59-61
- Rossi P.P. and Recupero A. (2013), “Ultimate strength of reinforced concrete circular members subjected to axial force, bending moment and shear force”, *ASCE J. Struct. Eng.*, **139**(6), 915-928.
- Russo G. and Puleri G. (1997), “Stirrup effectiveness in reinforced concrete beams under flexure and shear”, *ACI Struct. J.*, **94**(3), 451-476.
- Russo G., Somma G. and Angeli P. (2004), “Design shear strength formula for high strength concrete beams”, *Mater. Struct.*, **37**(274), 680-688.
- Russo G., Venier R., Pauletta M. (2005), “Reinforced concrete deep beams-shear strength model and design formula”, *ACI Struct. J.*, **102**(3), 429-437.
- Spinella N., Colajanni P. and Recupero A. (2010), “A simple plastic model for shear critical SFRC beams”, *ASCE J. Struct. Eng.*, **136**(4), 390-400.
- Spinella, N., Colajanni, P. and La Mendola, L. (2012), “Nonlinear analysis of beams reinforced in shear with stirrups and steel fibers”, *ACI Struct. J.*, **109**(1), 53-64.
- Spinella N. (2013), “Shear strength of full-scale steel fibre-reinforced concrete beams without stirrups”, *Comput. Concr.*, **11**(5), 365-382.
- Tan, K.H. and Ng, C.K. (1998), “Effect of shear in externally prestressed beams”, *ACI Struct. J.*, **95**(2), 116-128.
- Thürlimann, B., Marti, P., Pralong, J., Ritz, P. and Zimmerli, B. (1983), “Anwendung der plastizitätstheorie

- auf stahlbeton, institut für Baustatik und konstruktion”, ETH Zürich, Autographie zum Fortbildungskurs.
- Vecchio, F.J. and Collins, M.P. (1986), “The modified compression field theory for reinforced concrete elements subjected to shear”, *ACI Struct. J.*, **83**(2), 219-231.
- Vecchio, F.J. (2000), “Disturbed stress field model for reinforced concrete: Formulation”, *ASCE J. Struct. Eng.*, **126**(9), 1070-1077.
- Wong, P.S. and Vecchio, F.J. (2002), “VecTor2 and form works users manual”, *Technical report. Department of Civil Engineering*, University of Toronto – Canada.
- Vecchio, F.J. and Collins M.P. (1982), “Response of reinforced concrete to in plane shear and normal stress”, *Technical report, Department of Civil Engineering*, University of Toronto – Canada.

Symbols

A_{jf}	longitudinal flange reinforcement ($j = t, b$ with $t = \text{top}$ and $b = \text{bottom}$)
A_l	longitudinal web reinforcement
A_w	transversal web reinforcement
b_w	web width
$f_{cd1} = 0.85(1-f_{ck}/250)(f_{ck}/\gamma_c)$	design strength of concrete, for long period uniaxial load (f_{ck} in MPa)
$f_{cd2} = 0.60(1-f_{ck}/250)(f_{ck}/\gamma_c)$	design strength of concrete, in presence of transversal load (f_{ck} in MPa)
f_{ck}	characteristic strength of concrete
f_{yd}	design yield strength of ordinary steel reinforcement
f_{pd}	design strength of steel prestressing tendons
l	length of region
M_{Rd}	resisting bending moment
M_{Sd}	design bending moment
P	load capacity of specimen
R_i	region of beam ($i = 1, 2, 3$)
S	area of whole cross-section
S_{jf}	area of flange ($j = t, b$ with $t = \text{top}$ and $b = \text{bottom}$)
S_{wi}	area of web layers ($i = 1, 2, 3$)
s	spacing of transversal web reinforcement
t	thickness of region
V_{Rd}	resisting shear force
V_{Sd}	design shear force
z_i	depth of web layers ($i = 1, 2, 3$)
α_i	angle of the i th tendon on the longitudinal direction
δ	midspan displacement of specimen
γ_c	partial safety factor for concrete
γ_s	partial safety factor for steel
θ	angle of compressive stress field on the longitudinal direction
$\rho_{jf} = A_{jf}/S_{jf}$	longitudinal flange reinforcement ratio ($j = t, b$ with $t = \text{top}$ and $b = \text{bottom}$)
ρ_{sx}, ρ_{sy}	longitudinal and transversal reinforcement ratio
$\rho_{wl} = A_w/b_w h_w$	longitudinal web reinforcement ratio
$\rho_{wt} = A_w/b_w s$	transversal web reinforcement ratio
σ_{jf}	axial stress in flange layers ($j = t, b$ with $t = \text{top}$ and $b = \text{bottom}$)
σ_{pi}	axial stress in the i th tendon
σ_{wi}	axial stress in web layers ($i = 1, 2, 3$)
τ	shear stress in the central web layer
$\omega_{fl} = (A_{tf} + A_{bf}/S)(f_{yd}/f_{cd1})$	total longitudinal flange reinforcement mechanical ratio
$\omega_l = (A_l/b_w h_w)(f_{yd}/f_{cd1})$	longitudinal web reinforcement mechanical ratio
$\omega_w = (A_w/b_w s)(f_{yd}/f_{cd2})$	transversal web reinforcement mechanical ratio

A. APPENDIX

The failure of the structural element may occur either by concrete crushing or by reinforcements yielding. Using the design values given by Eurocode (2002) for steel yielding f_{yd} and for concrete compression strength f_{cd1} and f_{cd2} , the following conditions are obtained:

In the top and bottom flange layers

$$-(f_{cd1} + \rho_{tf} f_{yd}) \leq \sigma_{tf} \leq \rho_{tf} f_{yd} \quad (\text{A.1a})$$

$$-(f_{cd1} + \rho_{bf} f_{yd}) \leq \sigma_{bf} \leq \rho_{bf} f_{yd} \quad (\text{A.1b})$$

In the outermost web layers

$$-(f_{cd1} + \rho_l f_{yd}) \leq \sigma_{w1} \leq \rho_l f_{yd} \quad (\text{A.2a})$$

$$-(f_{cd1} + \rho_l f_{yd}) \leq \sigma_{w2} \leq \rho_l f_{yd} \quad (\text{A.2b})$$

In the central web layer

$$-(\sigma_{w3} + \rho_l f_{yd}) \tan \vartheta \leq \tau \leq -(\sigma_{w3} + \rho_l f_{yd}) \tan \vartheta \quad (\text{A.3a})$$

$$\tau \leq \rho_w f_{yd} \cot \vartheta \quad (\text{A.3b})$$

$$\tau \leq f_{cd2} \sin \vartheta \cos \vartheta \quad (\text{A.3c})$$

Furthermore, each prestressing tendon is subjected to an axial force, acting with an angle of α_i degrees to the longitudinal direction, which is taken into account separately from the aforementioned stress fields. The stress in the i th tendon is limited by the condition:

$$\sigma_{pi} \leq f_{pd} \quad (\text{A.4})$$

The resultants of axial and shear stress, plus the effect of the forces acting on the prestressing tendons, provide the resisting internal actions of the cross section, bending moment M_{Rd} and shear force V_{Rd} (while axial force N_{Rd} is null):

$$M_{Rd} = \int_S \sigma y dS + \sum_{n_p} A_{pi} y_{pi} \sigma_{pi} \cos \alpha_i \quad (\text{A.5a})$$

$$V_{Rd} = \int_{S_{w3}} \tau dS + \sum_{n_p} A_{pi} y_{pi} \sigma_{pi} \sin \alpha_i \quad (\text{A.5b})$$

$$N_{Rd} = \int_S \sigma dS + \sum_{n_p} A_{pi} y_{pi} \sigma_{pi} \cos \alpha_i = 0 \quad (\text{A.5c})$$

In the previous equations, the terms related to the areas S_{w1} , S_{w2} , and S_{w3} depend on the depth of the web layers z_1 , z_2 , and z_3 , which may vary according to the following geometrical and static conditions:

$$z_1 \geq 0 \quad (\text{A.6a})$$

$$z_2 \geq 0 \quad (\text{A.6b})$$

$$z_1 + z_2 + z_3 = h_w \quad (\text{A.6c})$$

$$z_3 \geq z_{3min} \quad (\text{A.6d})$$

In particular, Eq. (A.6d) states that the central web layer depth must be sufficient to bear shear stresses; its minimum value z_{3min} , which depends on concrete strength f_{cd2} and on transverse web reinforcement

mechanical ratio ω_t , is given by:

$$z_{3\min} = \frac{V_{Sd}}{f_{cd} b_w \sqrt{\omega_t (1 - \omega_t)}} \quad \text{if} \quad \omega_t \leq 0.5 \quad (\text{A.7a})$$

$$z_{3\min} = \frac{2V_{Sd}}{f_{cd} b_w} \quad \text{if} \quad \omega_t > 0.5 \quad (\text{A.7b})$$

The web depth h_w has to be greater than $z_{3\min}$ to satisfy the shear stress equilibrium. In case $z_{3\min} > h_w$ the web of the beam is not sufficient to sustain the shear stress and part of flange can be assumed to sustain shear stress in place of longitudinal stress, but in any case $z_{3\min}$ cannot be greater than the full depth of cross-section without enlarging the cross-section width.